

# Measurement of radio-frequency temporal phase modulation with chirped optical pulses

Michał Jachura,\* Jan Szczepanek, Wojciech Wasilewski, and Michał Karpiński

*Faculty of Physics, University of Warsaw,*

*Pasteura 5, 02-093 Warszawa, Poland*

## Abstract

We present an optical method to measure radio-frequency electro-optic phase modulation profiles by employing spectrum-to-time mapping realized by highly chirped optical pulses. We directly characterize temporal phase modulation profiles of up to 12.5 GHz bandwidth, with temporal resolution comparable to high-end electronic oscilloscopes. The presented optical setup is a valuable tool for direct characterization of complex temporal electro-optic phase modulation profiles, which is indispensable for practical realization of deterministic spectral-temporal reshaping of quantum light pulses.

arXiv:1706.09881v1 [physics.ins-det] 27 Jun 2017

---

\* [michal.jachura@fuw.edu.pl](mailto:michal.jachura@fuw.edu.pl)

## I. INTRODUCTION

Encoding of quantum information in the spectral-temporal degree of freedom of optical pulses has been recently recognized as a promising platform for high-dimensional quantum information processing and quantum communication, that is naturally compatible with fiber-optic infrastructure and integrated optical setups [1–3]. Realization of general spectral-temporal photonic quantum information processing and measurement requires spectral-temporal shaping of optical pulses that does not involve spectral nor temporal filtering. A recipe for such manipulations is well-known within the field of classical ultrashort pulse shaping [4–6]. It relies on successive imprinting spectral and temporal phase onto the optical pulse in a controllable manner. While the former is achieved simply by propagating the pulse through a dispersive medium, the latter requires elaborate active modulation techniques, which may be implemented e. g. by nonlinear-optical [6–10] or electro-optic methods [11–14]. The substantial advantage of electro-optic, and the recently demonstrated electro-optomechanical approach [15], lies in its low-noise and deterministic operation, which are key characteristics for applications in optical quantum technologies [14–17].

In the electro-optic approach a well-defined temporal phase imprint is applied to the optical pulse, which is realized by driving an electro-optic phase modulator (EOPM) by an appropriate radio-frequency (RF) field, with bandwidths reaching up to tens of GHz. Detailed characterization of the imprinted temporal phase becomes thus a key necessity, especially given recent efforts to diversify from standard single-tone RF modulation techniques [11, 15, 16, 18] to more complex temporal phase profiles [12, 13, 19], in particular in guided-wave electronic systems. Here we experimentally show the reconstruction of a fast temporal phase modulation profile performed using the spectral encoding method, a technique which is extensively employed in photonic time stretch (PTS) analysis of RF signals [20–22] as well as for detailed characterization of THz frequency electric-field pulses [23–26].

We use a highly chirped optical pulse to probe the phase imprinted by a RF field applied to an EOPM. The spectral phase of the optical pulse is afterwards recovered using the interferometric Fourier-transform method [27, 28] and, after appropriate chirp calibration, translated into the temporal profile of the modulating pulse with temporal resolution comparable to or surpassing the fastest electronic oscilloscopes available. The temporal phase modulation profiles are directly probed without the need for electro-optic response

calibration of the EOPM. Its calibration can be optionally employed to translate the phase modulation profile into the electronic waveform inducing it, which effectively turns the setup into a high-bandwidth optical oscilloscope.

Compared with hitherto reported experiments within the spectral encoding framework our work is related to the scheme presented in ref. [23], where free-space THz waveforms were characterized. We extend the applications of THz-pulse-characterization methods to direct measurement of radio-frequency temporal phase modulation profiles in a guided-wave platform. Since our solution can also be employed for the reconstruction of RF signals themselves, it can be alternatively treated as a variation of PTS technique relying on phase rather than intensity modulation of a chirped optical pulse.

## II. MEASUREMENT SCHEME

Our experimental implementation relies on a Mach-Zehnder interferometer with a lithium-niobate-waveguide EOPM placed in one of its arms and a variable delay line  $\tau$  placed in the other arm. The interferometer is fed with heavily chirped optical pulses and one of its output ports is monitored by a spectrometer, such as an optical spectrum analyser (OSA). Assuming the temporal mismatch between interferometer arms  $\tau$ , and the spectral phase imprint resulting from temporal RF modulation  $\varphi(\omega)$  through time-to-frequency mapping induced by the pulse chirp, the spectral intensity of the output field is given by:

$$\begin{aligned} I(\omega) &\propto |E(\omega) + E(\omega)e^{i\omega\tau+i\varphi(\omega)}|^2 = \\ &= 2|E(\omega)|^2 + 2|E(\omega)|^2 \cos(\omega\tau + \varphi(\omega)), \end{aligned}$$

where  $E(\omega)$  is the initial spectral amplitude of the pulse entering the interferometer. In the Fourier domain, the two terms in the above equation correspond to three distinct peaks, i. e. the baseband peak and two symmetrically located sidebands. By choosing one of the sidebands, performing an inverse Fourier transform and subtracting the linear phase term one can recover the spectral phase profile  $\varphi(\omega)$  [27, 28], which is a standard phase retrieval method used e. g. in spectral interferometry for femtosecond pulse characterization [29]. The method requires calibrating the value of  $\tau$ , which we determine by retrieving the linear phase profile  $\omega\tau$  with RF modulation switched off. Once the value of  $\tau$  is known the RF waveform can be recovered from a single spectral measurement. Provided the pulses entering the

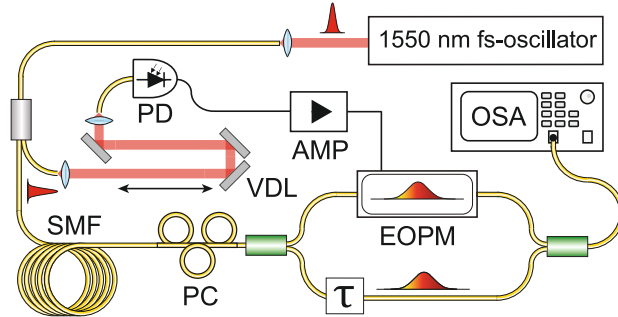


FIG. 1. Schematic representation of the experimental setup. DL, delay line, PD, photodiode, AMP, amplifier, EOPM, electro-optic phase modulator, SMF, single mode fiber, PC, polarization controller, OSA, optical spectrum analyser, VDL;  $\tau$ , variable delay lines.

interferometer are chirped such that temporal far-field condition is satisfied [5], the spectral phase  $\varphi(\omega)$  can be directly translated into the temporal profile of RF modulation using the linear relation  $\omega = \omega_0 + at$ , where  $a$  is the chirping rate and  $\omega_0$  is the central angular frequency of the pulse. Both parameters can be easily determined experimentally as we detail further in the text.

### III. EXPERIMENTAL SETUP

The scheme of our experimental setup is presented in Fig. 1. We use a polarization-maintaining-fiber Mach-Zehnder (MZ) interferometer with the EOPM placed in one of its arms. Alternatively a common-path polarization interferometer could be used [23, 30], provided the residual modulation of the orthogonal polarization component in the EOPM is appropriately taken into account. A pulsed beam from a fiber femtosecond oscillator (Menlo Systems C-Fiber HP, 1550 nm central wavelength, 50 fs pulse duration) is fiber-coupled and divided in two parts, of which one is sent through a free-space variable delay line and coupled into a 12.5 GHz bandwidth photodiode detector (PD, EoTech-3500FEXT), generating the RF pulse to be characterized, while the other is chirped in a length of single-mode fiber (SMF) and directed into the MZ interferometer. The RF pulse generated by the PD is amplified by a pair of broadband (0 – 40 GHz) RF amplifiers connected in series and fed into the EOPM (EO-Space PM-DV5-40-PFU-PFU-LV-UL) placed in one of the interferometer arms. Inside the EOPM the RF pulse temporally overlaps with the optical pulse chirped

during the propagation through either 250 m or 500 m of SMF (Corning SMF-28). The relative position between RF and optical pulse is tuned using 1.5 m-length air-gap variable delay line placed before the PD.

One of the output ports of the interferometer is monitored by an OSA (Yokogawa AQ6370D) whereas the second output port is sent through a bandpass filter (3 nm full-width-half-maximum bandwidth) and directed to an auxiliary photodiode detector (not presented in the experimental setup scheme). Simultaneous monitoring of interference fringes in the spectral and temporal domains simplifies the initial alignment of the interferometer in a balanced position, which facilitates the temporal synchronization between the RF and optical pulses. For the actual measurements the interferometer is used in an unbalanced setting, with only the OSA being monitored.

#### IV. RESULTS AND DISCUSSION

In Fig. 2 we present exemplary interferometer output spectra ( $\tau \neq 0$ ) collected using the OSA with RF modulation switched off and on for the case of 250 m-long chirping SMF. The phase imprinted by the RF pulse significantly modifies the positions of minima and maxima of spectral interference fringes over approximately 50 nm bandwidth range. In further experiments we used larger values of  $\tau$ , resulting in more dense spectral fringes, which allowed us to easily separate one of the spectrum sidebands after its transformation into the Fourier domain. In our experiment the acquisition time of a single OSA measurement is much longer than the time interval between two subsequent optical pulses. Single shot acquisition could be achieved by employing a spectrometer with a multipixel detector array

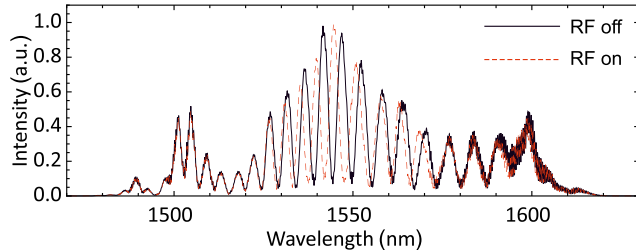


FIG. 2. Exemplary interferometer output spectra measured by the OSA for  $\tau \neq 0$ , with and without RF phase modulation.

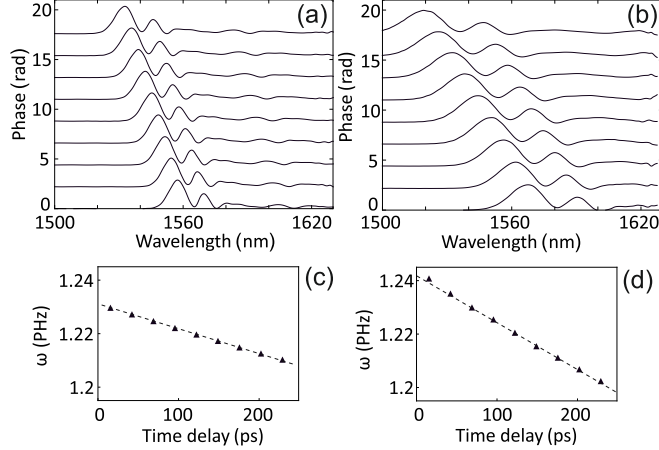


FIG. 3. Phase modulation profiles retrieved for a series of different delays between the RF waveform and the optical pulse. The maxima of the waveforms are traced to recover the SMF group delay dispersion value yielding  $-11.1 \text{ ps}^2$  for 500 m of SMF (a, c) and  $-5.73 \text{ ps}^2$  for 250 m of SMF (b, d).

and reducing the repetition rate of the fs oscillator to match the spectrometer refresh rate (e. g. by an external pulse picker) [28, 30]. Alternatively, in analogy to the PTS approach, frequency-to-time mapping via the dispersive Fourier transform principle could be used to record the spectrum using a single fast photodiode [20], possibly with an appropriate reduction of repetition rate.

To retrieve the chirp value  $a$  and verify the repeatability of our measurement scheme we retrieved the phase modulation profiles for a series of relative positions between the RF waveform and the optical pulse. This has been achieved by adjusting the air-gap variable delay line in a series of 4 mm steps corresponding to 13.34 ps of delay. In Fig. 3(a,b) we present the result of this procedure for the 250 m and 500 m lengths of the chirping SMF. The position of modulation maximum has been recorded to recover the SMF group delay dispersion values yielding  $-11.1 \text{ ps}^2$  for 500 m of SMF, Fig. 3(c), and  $-5.73 \text{ ps}^2$  for 250 m of SMF, Fig. 3(d).

The final result of the experiment is shown in Fig. 4, where we present the RF modulation profiles retrieved for the two values of optical pulse chirp, Fig. 4(a). The reconstructed waveforms agree very well with each other. Naturally the temporal interval covered by the chirped optical pulse is longer for a larger GDD value. We verified that the sensitivity of our setup allows to measure pulses generated directly by the PD with a peak voltage of 100 mV.

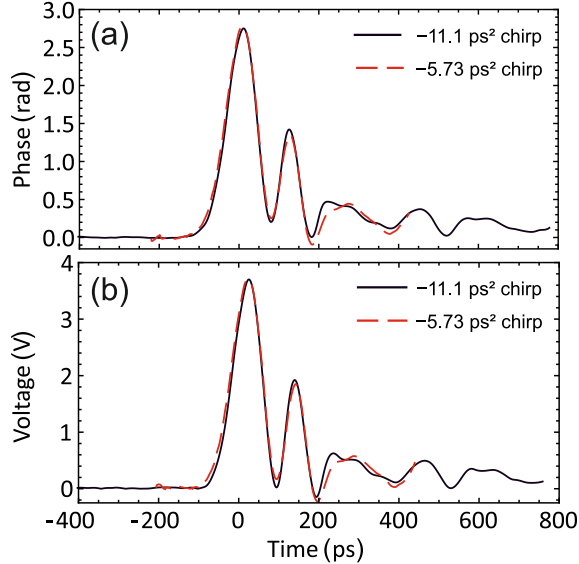


FIG. 4. Retrieved RF temporal phase modulation profile (a), and the corresponding electronic waveform profile (b) for the two values of optical pulse chirp (solid and dashed lines).

For the purpose of spectral-temporal light shaping the most relevant information is the temporal phase modulation profile induced by the RF pulse. It can however be converted to retrieve the actual electronic waveform by using the EOPM electro-optic response profile. The response profile of our EOPM has been characterized in the 0 – 30 GHz frequency range with the half-wave voltage of 4 V at 1 GHz modulation frequency. In the temporal domain the measured phase modulation profile is a convolution of the electronic signal feeding the EOPM with its electro-optic response function. Thus the retrieval of electronic waveform requires a reciprocal deconvolution operation, which is especially easy to implement in the spectral domain, where it corresponds to division by the EOPM spectral response function. The division performed in the spectral domain is also beneficial for the deconvolution fidelity since this is the domain where instrument response function is directly measured. The results of the deconvolution procedure, based on the measured spectral response profile provided by the EOPM manufacturer, are presented in Fig. 4(b).

The temporal resolution achievable through chirped-pulse spectral-temporal mapping is given by  $(t_b t_a)^{1/2}$ , where  $t_b$  and  $t_a$  are the duration of the optical pulse before and after the chirp [31]. For the optical pulses employed in our setup this value equals approximately 8.7 ps for 500 m and 6.1 ps for 250 m of SMF. Although the expected optical temporal resolution can

easily reach single ps, in practice the resolution is limited by the finite bandwidth of EOPMs. Whereas this limitation is irrelevant for the direct characterization of phase-modulation profiles, for probing of electronic waveforms it imposes a trade-off between the sensitivity and temporal resolution of the method, as the EOPM bandwidth could be increased at the cost of reduced sensitivity by using a shorter modulator. This can be mitigated by the development of novel types of electro-optic modulators offering both exceptionally low half-wave voltage and high modulation bandwidth [32, 33].

## V. CONCLUSIONS AND OUTLOOK

We present a robust method for the direct characterization of RF temporal phase modulation profiles by means of chirped-pulse electro-optic sampling method. It extends the applications of THz field characterization methods and spectral encoding techniques to radio-frequency temporal phase profiles in an integrated optical platform, which are routinely employed for electro-optic spectral shaping of classical and quantum light. Alternatively it can be used for the reconstruction of RF electronic signals inducing phase modulation, which presents a variation of the PTS technique relying on phase rather than intensity modulation, involving a phase-sensitive detection scheme. Our work paves the way towards deterministic realization of complex spectral-temporal mode transformations, including general unitary transformations [34], which will lead to important developments in spectrally-encoded photonic quantum information processing and communication [1]. Thanks to the reconfigurability of electro-optic phase modulation patterns we also expect it to become an valuable tool in realization of adaptive spectral-temporal shaping strategies, in particular of quantum light [35].

## VI. ACKNOWLEDGEMENTS

We thank K. Banaszek and C. Radzewicz for careful reading of the manuscript. This work has been supported by the National Science Centre of Poland (project no. 2014/15/D/ST2/02385).

The authors declare that they have no conflict of interest.

---

- [1] Brecht, B.; Reddy, D. V.; Silberhorn, C.; Raymer, M. G., *Phys. Rev. X* **2015**, *5*, 041017.
- [2] Humphreys, P. C.; Metcalf, B. J.; Spring, J. B.; Moore, M.; Jin, X. M.; Barbieri, M.; Kolthammer, W. S.; Walmsley, I. A., *Phys. Rev. Lett.* **2013**, *111*, 150501.
- [3] Lukens, J.M.; Lougovski, P., *Optica* **2017**, *4*, 8–16.
- [4] Agrawal, G.P. *Fiber-Optic Communication System* **2010**, Wiley.
- [5] Torres-Company, V.; Lancis, J.; Andrés, P. *Prog. Opt.* **2011**, *56*, 1–80.
- [6] Salem, R.; Foster, M.A.; Gaeta, A.L. *Adv. Opt. Photonics* **2013**, *5*, 274–317.
- [7] Agha I., Ates S., Sapienza L., Srinivasan K., *Opt. Lett.* **2014**, *39*, 5677–5680
- [8] Zhu, Y.; Kim, J.; Gauthier, D.J.; *Phys. Rev. A* **2013**, *87*, 043808.
- [9] Donohue, J.M.; Mastrovich, M.; Resch, K.J. *Phys. Rev. Lett.* **2016**, *117*, 243602.
- [10] Matsuda, N., *Science Adv.* **2016**, *2*, e1501223.
- [11] Karpiński, M.; Jachura, M.; Wright, L.J.; Smith, B.J. *Nat. Photon.* **2016**, *11*, 53–57.
- [12] Li, B.; Li, M.; Lou, S.; Azaña, J. *Opt. Express* **2013**, *21*, 16814–16830.
- [13] Poberezhskiy, I. Y.; Bortnik, B.; Chou, J.; Jalali, B.; Fetterman, H. R. *IEEE J. Quant. Electron* **2005**, *41*, 1533-1539.
- [14] Wright, L.J.; Karpiński, M.; Söller, C.; Smith, B.J., *Phys. Rev. Lett.* **2017**, *118*, 023601.
- [15] Fan, L.; Zou, C.-l.; Poot, M.; Cheng, R.; Guo, X.; Han, X.; Tang, H. X. *Nat. Photon.* **2016**, *10*, 766-770.
- [16] Olislager, L.; Mbodji, I.; Woodhead, E.; Cussey, J.; Furfaro, L.; Emplit, P.; Massar, S.; Huy, K. P.; Merolla, J.-M. *New J. Phys.* **2012**, *14*, 043015.
- [17] Lukens, J. M.; Odele, O. D.; Leaird, D. E.; Weiner, A. M. *Opt. Lett.* **2015**, *40*, 5331-5334.
- [18] Plansinis, B. W.; Donaldson, W. R.; Agrawal, G. P. *J. Opt. Soc. Am. B* **2015**, *32*, 1550-1554.
- [19] Pedrotti, L. M.; Agha, I. *Opt. Express* **2016**, *24*, 16687-16694.
- [20] Coppinger, F.; Bhushan, A.S.; Jalali, B. *IEEE Trans. Microw. Theory Tech.* **1999**, *47*, 1309-1314.
- [21] Chou, J.; Boyraz, O.; Solli, D.; Jalali, B. *Appl. Phys. Lett.* **2007**, *91*, 161105.
- [22] Buckley, B. W.; Madini, A.M.; Jalali, B. *Opt. Express* **2013**, *21*, 21618-21627.
- [23] Jiang, Z.; Zhang, X.-C. *Appl. Phys. Lett.* **1998**, *72*, 1945-1947.

- [24] Yan, X.; MacLeod, A.M.; Gillespie, W.A.; Knippels, G.M.H.; Oepts, D.; van der Merr, A.F.G.; Seidel, W.; *Phys. Rev. Lett.* **2000**, *85*, 3404–3407.
- [25] Matlis, N.H.; Plateau, G.R.; van Tilborg, J.; Leemans, W.P. *J. Opt. Soc. Am. B* **2011**, *28*, 23–27.
- [26] Roussel, E.; Evain, C.; Parquier, M.L.; Szwaj, C.; Bielawski, S.; Manceron, L.; Brubach J.-B.; Tordeaux, M.-A.; Ricaud, J.-P.; Cassinari, L.; Labat, M; Couprie, M.-E.; Roy, P. *Sci. Rep.* **2015**, *5*, 10330.
- [27] Takeda, M.; Ina, H.; Kobayashi, S. *J. Opt. Soc. Am. A* **1982**, *72*, 156–160.
- [28] Zhou, M.-L.; Feng, L.; Chun, L.; Fei, D.; Li, Y.-T.; Wang, W.-M.; Sheng, Z.-M.; Chen, L.-M.; Ma, J.-L.; Lu, X.; Dong, Q.-L.; Zhang, J. *Chin. Phys. Lett* **2012**, *29*, 015202.
- [29] Iaconis, C.; Walmsley, I. A. *IEEE J. Quant. Electron* **1999**, *35*, 501–509.
- [30] Kim, K. Y.; Yellampalle, B.; Rodriguez, G.; Averitt, R. D.; Taylor, A. J.; Glowonia, J. H. *Appl. Phys. Lett.* **2006**, *88*, 041123.
- [31] Sun, F. G.; Jiang, Z.; Zhang, X.-C. *Appl. Phys. Lett.* **1998**, *73*, 2233–2235.
- [32] Enami, Y.; Mathine, D.; DeRose, C. T.; Norwood, R. A.; Luo, J.; Jen, A. K.-Y.; Peyghambarian, N. *Appl. Phys. Lett.* **2007**, *91*, 093505.
- [33] Melikyan, A.; Alloatti, L.; Muslija, A.; Hillerkuss, D.; Schindler, P. C.; Li, J.; Palmer, R.; Korn, D.; Muehlbrandt, S.; Van Thourhout, D.; Chen, B.; Dinu, R.; Sommer, M.; Koos, C.; Kohl, M.; Leuthold, J. *Nat. Photon.* **2014**, *8*, 229–233.
- [34] Morizur, J.-F.; Nicholls, L.; Jian, P.; Armstrong, S.; Treps, N.; Hage, B.; Hsu, M.; Bowen, W.; Janousek, J.; Bachor, H.-A. *J. Opt. Soc. Am. A* **2010**, *27*, 2524–2531.
- [35] Polycarpou, C.; Cassemiro, K. N.; Venturi, G.; Zavatta, A.; Bellini, M. *Phys. Rev. Lett.* **2012**, *109*, 053602.